Available online at www.sciencedirect.com
SCIENCE DIRECT®
ELSEVIER
Mechanical Systems and Signal Processing 20 (2006) 1221–1238
Mechanical Systems and Signal Processing
www.elsevier.com/locate/jnlabr/ymssp

Fault diagnosis in machine tools using selective regional correlation

Adam G. Rehorn, Ervin Sejdić, Jin Jiang*

Department of Electrical and Computer Engineering, The University of Western Ontario, London, Ont., Canada N6A 5B9

Received 4 August 2004; received in revised form 12 January 2005; accepted 19 January 2005
Available online 23 March 2005

Abstract

This paper investigates the detection and diagnosis of brush seizing faults in the spindle positioning servo drive of a high-precision machining centre using a recently developed time–frequency pattern classification technique known as selective regional correlation (SRC). It is shown that SRC is capable of significantly enhancing the resolution of fault diagnosis when compared to conventional correlation-based techniques. The performance of this approach is evaluated using three time–frequency transformation techniques: the short-time Fourier transform (STFT), continuous wavelet transform (CWT) and S-Transform. In addition, three different 2D windows are used to isolate features for use with SRC: a rectangular (boxcar) window, a Gaussian window and a Kaiser window. The results have indicated that SRC is a promising tool for machine condition monitoring (MCM).

Keywords: Machine condition monitoring; Selective regional correlation; Time–frequency transformations; Pattern classification

1. Introduction

In manufacturing, there is an increasing demand for higher production rates, improved part quality and larger throughput volumes [1]; in short "faster, better and cheaper". Thus, there is a strong desire to move from the current state of manufacturing automation to total autonomy. To

*Corresponding author. Tel.: +1 519 661 2111 x 88320; fax: +1 519 850 2436.
E-mail addresses: agrehorn@uwo.ca (A.G. Rehorn), esejdic@uwo.ca (E. Sejdić), jjiang@uwo.ca (J. Jiang).

0888-3270/$ - see front matter
doi:10.1016/j.ymssp.2005.01.010

do so, effective monitoring and control of machining processes are required; degradations in machine tool performance must be detected and acted upon in a reliable and timely manner [2].

The issue of forced downtime, i.e. the time during which no machining operations are undertaken due to an undesirable event, is a major concern in manufacturing [2]. There are several different reasons for downtime, some of which are unavoidable, such as time for refixturing and setting up new production batches. However, downtime resulting from machine failures should, ideally, be eliminated.

To reach the goal of autonomy, interest in monitoring machining processes and systems, including tool condition monitoring (TCM) [1], has increased. Since the machine tool positioning and drive systems are crucial parts of a machine tool, their health is also critical for autonomous operations. Thus, it is very important to develop techniques for machine condition monitoring (MCM).

There exist a number of MCM methods in the literature. A time domain method is developed in [3], but it relies on mathematical models of the machines being monitored. In practice, the complexity of a machine tool system may prohibit comprehensive modeling. Neuro-fuzzy (NF) systems are investigated in [4], and are shown to be superior to recurrent neural networks (RNNs). Unfortunately, both approaches need training. This requires extra time and expense, and thus, is not feasible for MCM in an industrial environment. Frequency domain features have been extracted using bispectrum analysis in [5]. While successful, it requires resampling the vibration signal as a function of rotational speed, and thus needs a tachometer and additional computation.

Both wavelets and S-Transform-based schemes have been applied to the detection of gear wear in helicopter gearboxes [6,7]. It is shown that these time–frequency methods allow fault-related features to be detected. A review of wavelet-based MCM activities in [8] has identified several shortcomings, including a lack of standardisation in the choice of wavelets used for the analysis, and difficulties in interpreting the results of the wavelet transform.

Most approaches to MCM rely on the identification of features that are unique to a particular fault scenario. Often, this can take the form of a specific frequency component [9] or specific wavelet coefficients [4]. Identification of fault conditions follows directly through the recognition of these features. Correlation analysis, despite being very simple, is rarely used, as it is unsuitable for non-stationary signals. Difficulties arise, too, when the features that are indicative of a faulty condition do not exist in a unique frequency band. In some cases, as will be shown later, the signature of a faulty system contains the same frequency components as that of a healthy one. When this occurs, it can be very difficult to use the previously cited methods to monitor the health of the system.

Recently, a time–frequency domain based correlation technique, known as selective regional correlation (SRC), has been developed [10]. This method is potentially suitable for MCM because it is capable of identifying the state of health of a system even when the features of interest are represented by non-stationary signals across several frequency bands. By performing pattern matching and recognition only on the features of interest in the time–frequency domain and neglecting extraneous components, SRC can enhance correlation-based pattern recognition, particularly for MCM, thus simplifying the fault diagnostic process. In addition, SRC can be used with any time–frequency method, including the short-time Fourier transform, (STFT) [11,12], continuous wavelet transform (CWT) [12–14] and S-Transform [15,16], which increases its

flexibility considerably [10]. The procedure for calculating SRC is straightforward and can easily be automated, which makes it desirable in an industrial environment.

In this paper, the application of SRC to detecting a specific fault in a machine tool positioning drive is investigated, since brush seizing faults exhibit some unique characteristics in a frequency band for both healthy and faulty systems.

The main objective of the current study is to examine the performance of different time–frequency methods with SRC, to compare the performance of SRC-based MCM to that of conventional correlation-based MCM, and to show that the SRC approach is better suited for use in MCM applications. This is accomplished by: firstly, examining the nature of brush seizing faults through vibration analysis; secondly, identifying unique time–frequency domain signatures that represent this state of the machining system; thirdly, determining the performance of various time–frequency methods for use with SRC; finally, comparing the performance of SRC-based MCM with conventional correlation-based MCM. The main motivation is to develop a flexible and highly effective method suitable for automated MCM.

The main contribution of the paper is that a novel method for extraction and recognition of health-related features from machine tool vibration signals is developed based on SRC. The method is shown to be superior to other techniques using conventional correlation. Because SRC operates only on relevant features of interest, the number of required calculations is effectively reduced, and the speed and the accuracy of the recognition system has been improved considerably.

This paper is organised as follows: in Section 2, features of the vibration signals suitable for MCM are considered, and the concept of SRC is introduced; Section 3 discusses the experimental set-up as well as the nature of the fault and its vibrational signatures; Section 4 presents a measure for the performance of SRC and illustrates the effectiveness of SRC when applied to MCM analysis. Conclusions are drawn in Section 5, followed by acknowledgments and a list of references.

2. MCM and selective regional correlation

2.1. Features for MCM

In the main positioning system of a machine tool, there are many potential sources for mechanical failure. These include DC servomotor brush seizing, drive belt wear or stretching, and wear in the bearings and lead screws. Each of these problems exhibits a specific characteristic signature, and these signatures can be used for the purpose of MCM. The key is to identify a set of features that correspond unambiguously to either the healthy mode or the possible faulty modes of the machine. Such features can be found in vibration signals of the axes as they move during machining. By comparing the measured data to the failure signature, the state of the machine tool positioning drives can be determined.

In this paper, brush seizing faults in a DC servo motor drive that controls the position of the spindle block on the machine tool are used to illustrate the scheme and procedures. This fault originates from the design and construction of the brush holders, which are plastic and often warp with exposure to heat and lubricant. Whenever this happens, the spindle block experiences

excessive vibration. When one of the servos is faulty, the axis jumps along the guideways instead of moving smoothly. Experience has shown that this type of fault is incipient, and always leads to failure.

It has been found that, for a healthy spindle, there are no clear patterns in the vibration signals. However, periodic phenomena arise when a fault starts to develop in the system [17]. These phenomena become much more apparent in the time–frequency domain because they often appear as transient spikes of short duration. It is difficult to detect them in either the time domain or the frequency domain alone. This is because both the healthy and the faulty drives contain energy in the same frequency bands. However, there are increased periodic fluctuations with energy concentrated in the 20–200 Hz band when the system is faulty. Thus, a faulty system will exhibit a regular pattern of spikes in this frequency range, while a healthy one will not [17].

The features discussed above can always be observed in the vibrational signature of a faulty spindle block during translational motion, regardless of the direction or speed of motion, or the spindle rotational speed. Thus, by isolating these features, it is possible to determine the health of the spindle block positioning servo. It will be shown subsequently that SRC can reliably isolate these features from other signal components in the time–frequency domain and thus improve the accuracy of fault detection.

The basic idea behind SRC is to determine the similarity between a feature in a vibration signal from a machine in an unknown state, $v_U(t)$ and a feature that represents a known state of the machine. As mentioned previously, there are several potential faults that could occur. Let the signals that represent these fault conditions be $v_{Fi}(t)$, where $i = 1, 2, \ldots, n$, for n possible fault conditions. Since it is the faulty state vibrations that contain the features, $v_U(t)$ will be compared against $v_{Fi}(t)$. The strength of SRC is its ability to perform pattern matching using only a specific part of the time–frequency domain signal that contains pertinent information. Thus, the first step is to identify these characteristic features.

Let the time–frequency transforms of $v_U(t)$ and $v_{Fi}(t)$ be $Tv_U(\tau, \gamma)$ and $Tv_{Fi}(\tau, \gamma)$, respectively. From $Tv_{Fi}(\tau, \gamma)$, the features of interest can be isolated for fixed time and frequency bands $\tau \in [\tau_1, \tau_2]$ and $\gamma \in [\gamma_1, \gamma_2]$, respectively. The resulting isolated signal is referred to as the template signal, and is represented by $Tv_{Fi1}(\tau, \gamma)$. For the purpose of comparison, the same time and frequency ranges are applied to $Tv_U(\tau, \gamma)$, yielding $Tv_{U1}(\tau, \gamma)$, which is the isolated time–frequency representation of the features of interest in the observed signal.

Once suitably isolated, the signals with these features are transformed back to the time domain and the correlations between $v_{U1}(t)$ and the features $v_{Fi1}(t)$ can be determined. The $v_{Fi1}(t)$ that results in the highest correlation coefficient is then determined to represent the state of the machine. The general process of SRC-based fault diagnosis is shown in a block diagram form in Fig. 1. The specifics of SRC and the time–frequency methods used are explained in the section to follow.

2.2. Selective regional correlation: theoretical background

SRC is a scheme which can improve the performance of correlation-based pattern recognition for bandlimited, non-stationary signals. It is a time–frequency method that converts a one-dimensional (1D) time domain signal into a two-dimensional (2D) time–frequency domain representation. It allows correlation-based pattern matching to be conducted only in selected

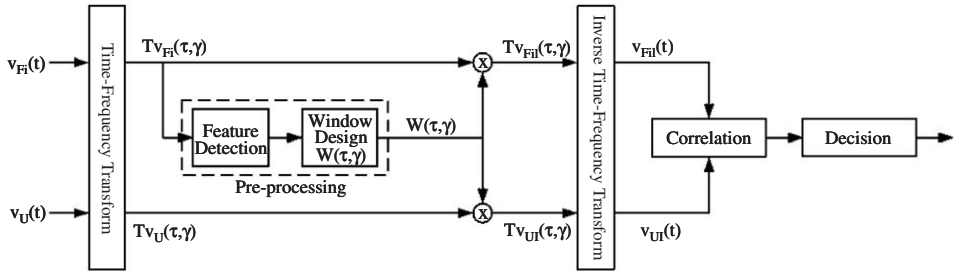

Fig. 1. Block diagram highlighting the steps of SRC-based fault diagnosis.

regions of interest in the time–frequency domain, thus reducing the number of calculations needed and improving the accuracy of the result [10]. The SRC algorithm consists of three main stages:

(1) Template selection in the time–frequency domain,
(2) Time–frequency domain pre-processing of the unknown signal, and
(3) Correlation of the unknown signal with the selected template.

Template selection is the most important step in SRC. If the signal containing the template is represented by $v_{Fi}(t) \in \mathbf{L}^2(R)$, its time–frequency transform can be evaluated by correlation with a function $\phi_{\tau,\gamma} \in \mathbf{L}^2(R)$ (known as the time–frequency atom [12]) that is well concentrated in time and frequency:

$$Tv_{Fi}(\tau,\gamma) = \int_{-\infty}^{\infty} v_{Fi}(t)\phi_{\tau,\gamma}(t)\,\mathrm{d}t. \tag{1}$$

Theoretically speaking, any time–frequency atom can be utilised in Eq. (1). However, due to the fact that signal decompositions are involved, bilinear class of time–frequency distributions, such as the Wigner distribution or Cohen's class [18], will be more computationally involved because of their cross product terms. In this paper, three different time–frequency transforms are considered: the STFT, CWT and S-Transform.

A short-time Fourier transform is a particular form of Eq. (1) with a window g which is translated by τ and modulated by γ [11,12]:

$$\phi_{\tau,\gamma}(t) = g_{\tau,\gamma}(t) = \mathrm{e}^{-j\gamma t}g(t-\tau). \tag{2}$$

A CWT is also a special case of Eq. (1) with dilation by γ and translation by τ of a mother wavelet ψ [12–14]:

$$\phi_{\tau,\gamma}(t) = \psi_{\tau,\gamma}(t) = \frac{1}{\sqrt{\gamma}}\psi\left(\frac{t-\tau}{\gamma}\right). \tag{3}$$

An S-Transform combines the short-time Fourier transform and the wavelet transform using a Gaussian window which is translated by τ, dilated and modulated by γ [15,16]:

$$\phi_{\tau,\gamma}(t) = g_{\tau,\gamma}(t) = \mathrm{e}^{-j\gamma t}g\left(\frac{t-\tau}{\gamma}\right). \tag{4}$$

Clearly, the S-Transform can be viewed from two different perspectives; as a short-time Fourier transform with a variable window length [15,16], or as a special type of CWT with a Gaussian mother wavelet modified by adding a phase factor [15,16]:

$$STv(\tau,\gamma) = \mathrm{e}^{-j2\pi\gamma\tau} CWTv(\tau,\gamma). \tag{5}$$

The time–frequency transform of the signal that bears the template, $Tv_{Fi}(\tau,\gamma)$, is the union of two components: the template, $Tv_{Fi1}(\tau,\gamma)$, and its complement, $Tv_{Fi2}(\tau,\gamma)$. Let us assume that the features representing the template are located in the time and frequency bands $\tau \in [\tau_1,\tau_2]$ and $\gamma \in [\gamma_1,\gamma_2]$, respectively. Thus

$$Tv_{Fi1}(\tau,\gamma) \equiv 0 \quad \forall\tau \notin [\tau_1,\tau_2],\ \gamma \notin [\gamma_1,\gamma_2]. \tag{6}$$

To extract $Tv_{Fi1}(\tau,\gamma)$ from the time–frequency representation $Tv_{Fi}(\tau,\gamma)$, a 2D window $W(\tau,\gamma)\,\forall\tau \in [\tau_1,\tau_2], \gamma \in [\gamma_1,\gamma_2]$ can be used:

$$Tv_{Fi1}(\tau,\gamma) = Tv_{Fi}(\tau,\gamma)\cdot W(\tau,\gamma), \quad \tau \in [\tau_1,\tau_2] \quad \text{and} \quad \gamma \in [\gamma_1,\gamma_2]. \tag{7}$$

In this paper, a three different 2D window functions are used. The first is a boxcar function, which is defined as follows:

$$W_b(\tau,\gamma) = \begin{cases} A & \forall\tau,\gamma \in R, \\ 0 & \text{otherwise.} \end{cases} \tag{8}$$

The second is a 2D Gaussian window, which is defined as

$$W_g(\tau,\gamma) = \begin{cases} \dfrac{1}{2\pi\sigma_\tau\sigma_\gamma}\mathrm{e}^{\frac{-\tau^2}{2\sigma_\tau^2}-\frac{-\gamma^2}{2\sigma_\gamma^2}} & \forall\tau,\gamma \in R, \\ 0 & \text{otherwise.} \end{cases} \tag{9}$$

The third is a 2D Kaiser window, given by

$$W_k(\tau,\gamma) = \begin{cases} \dfrac{I_0(\beta_\tau\sqrt{1-\tau^2})I_0(\beta_\gamma\sqrt{1-\gamma^2})}{I_0(\beta_\tau)I_0(\beta_\gamma)} & \forall\tau,\gamma \in R, \\ 0 & \text{otherwise,} \end{cases} \tag{10}$$

where β_τ and β_γ represent parameters that affect the sidelobe attenuation and $I_0(\cdot)$ is the zeroth-order modified Bessel function. The region of support for all three windows is given by $R = \{(\tau,\gamma) : \tau_1 \leqslant \tau \leqslant \tau_2,\ \gamma_1 \leqslant \gamma \leqslant \gamma_2\}$.

To obtain the time domain expression of the template signal, $v_{Fi1}(t)$, the inverse time–frequency transform can be used

$$v_{Fi1}(t) = \int_{-\infty}^{\infty}\int_{-\infty}^{\infty} Tv_{Fi1}(\tau,\gamma)K(\tau,\gamma,t)\,\mathrm{d}\tau\,\mathrm{d}\gamma, \tag{11}$$

where $K(\tau,\gamma,t)$ is the kernel for the inversion.

Once suitable templates are selected, the time–frequency pre-processing of the unknown signal, $v_U(t)$, can be carried out. The pre-processing involves forward time–frequency transform on $v_U(t)$ based on Eq. (1) (with the signal $v_{Fi}(t)$ in the integration replaced by $v_U(t)$).

The time–frequency representation of the unknown signal, $Tv_U(\tau,\gamma)$, is then multiplied by the 2D window function, $W(\tau,\gamma)$, to localise the feature space. The product is then converted back to the time domain using the inverse time–frequency transform presented in Eq. (11) (albeit with $Tv_{U1}(\tau,\gamma)$ replacing $Tv_{Fi1}(\tau,\gamma)$). This produces a time domain signal for comparison with the template in Eq. (11). This signal is represented as $v_{U1}(t)$.

Using the template and the windowed signals in the time domain, SRC can be performed and the result, $\rho_i(\zeta)$, the correlation coefficient between $v_{Fi1}(t)$ and $v_{U1}(t)$, can be calculated as follows:

$$\rho_i(\zeta) = \left| \frac{\int_{-\infty}^{\infty} v_{Fi1}(t) v_{U1}(t+\zeta)\,\mathrm{d}t}{\sqrt{\int_{-\infty}^{\infty} v_{Fi1}(t)^2\,\mathrm{d}t}\sqrt{\int_{-\infty}^{\infty} v_{U1}(t)^2\,\mathrm{d}t}} \right|. \tag{12}$$

The peak magnitude of $\rho_i(\zeta)$ indicates the similarity between the signal in the time–frequency region of interest and the ith template. This variable will be used later for fault detection purposes.

3. Faults and their signatures

3.1. Experimental set-up

The machine tool used in this investigation is a Proteo D/94 high-precision machining centre. This is a five axis machining system, the general arrangement of which can be seen in Fig. 2. The spindle block is mounted along the Z-axis. It is the positioning drive servo of the Z-axis that is prone to brush seizing.

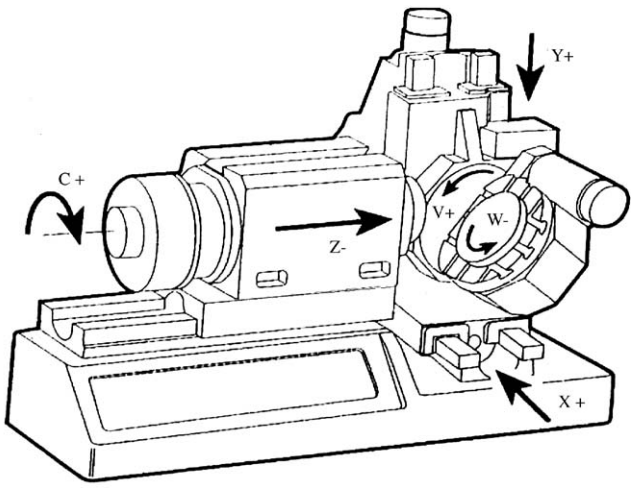

Fig. 2. General arrangement of the Proteo D/94 5-axis machining centre.

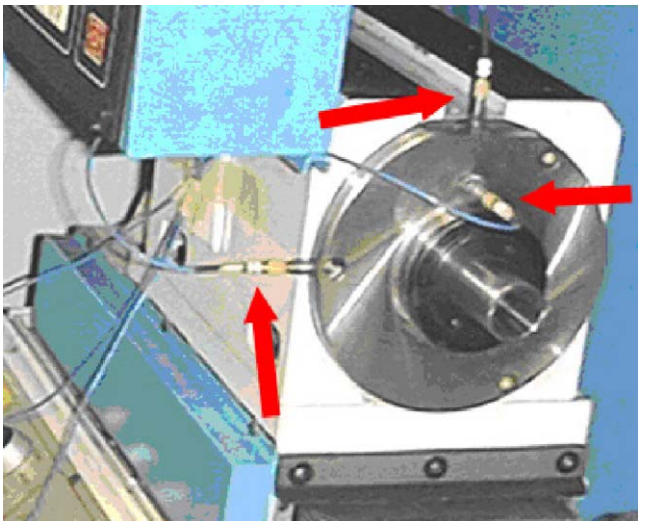

Fig. 3. Mounting of the three accelerometers on the D/94 spindle block. Arrows indicate sensor locations.

To measure the vibrations of the spindle during translation, three PCB Piezotronics model 352C68 piezoelectric accelerometers (frequency range 0.3–12 000 Hz, max. acceleration = 490 m/s^2) are mounted to the spindle block in the X, Y and Z directions, as seen in Fig. 3. These sensors are chosen because they are easy to install and use, and are robust enough to survive in an industrial setting [1,19]. They do not require extensive refitting or modification to the machine tool, nor do they change the dynamics of the system.

Measurements with a faulty positioning drive are taken first. This drive is then replaced with a healthy motor from the same manufacturer, and the same tests are performed. The spindle is translated in the positive (away from the workpiece) and negative (toward the workpiece) direction at 100, 10 and 1 percent of the rated feed speed. Twelve tests are conducted for each of the healthy and the faulty systems. Of these tests, six are conducted with the spindle stationary, while the rest are performed with the spindle running at 1995 and 2300 rpm. The vibration signals are recorded using an HP35670A dynamic signal analyser with a sampling frequency of 4096 Hz.

3.2. *Nature of the fault*

As mentioned in Section 2.1, there are several potential faults that could occur in the drive system along the various axes of the D/94. However, in this paper, the results presented are only those relating to a brush seizing fault in the spindle positioning drive servo. The vibrations of a healthy and a faulty motor are presented in Figs. 4 and 5, respectively. It can be seen that, while there are differences in the patterns in the time domain, it is difficult to determine which set of data represents a healthy and which a faulty drive. Thus, time domain thresholding is not viable for MCM in this case. Frequency domain analysis of the data reveals that the two signals share many frequency components. There are no unique features that can be extracted from either the time or the frequency domain to distinguish a healthy motor from a faulty one.

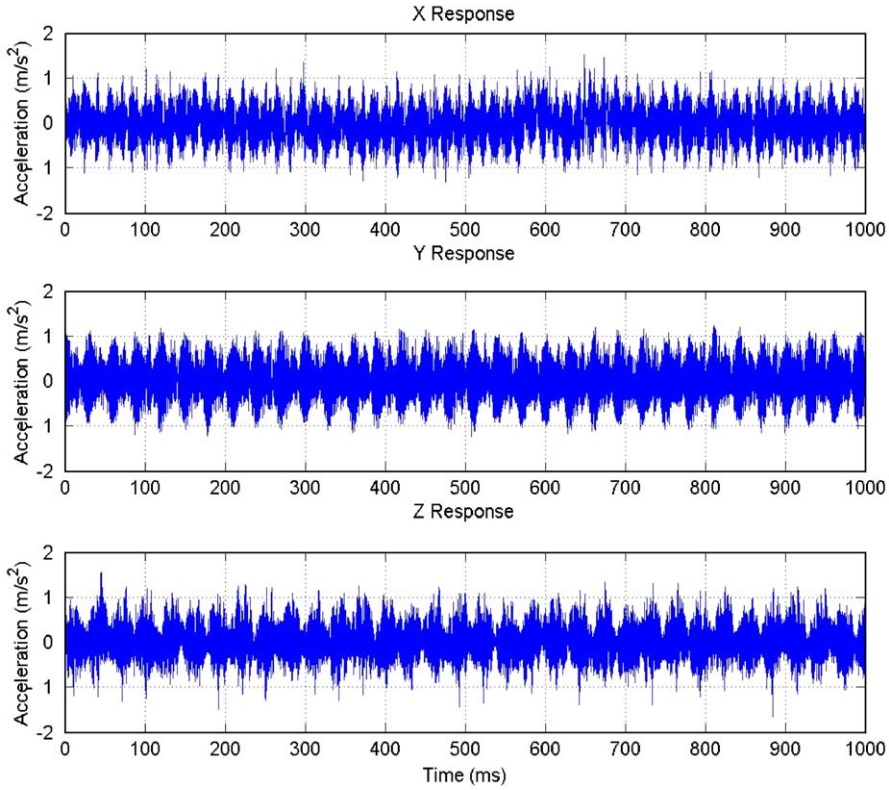

Fig. 4. Vibrations of the spindle block with a healthy positioning drive.

3.3. Failure signatures in the time–frequency domain

As mentioned in the Introduction, the analysis of the collected vibration data can be performed in the time–frequency domain using three transforms: the STFT, CWT and S-Transform. Fig. 6 presents the STFT, CWT and S-Transform for the same signal; the vibrations in the X direction with a brush seizing fault.

As will be shown, the S-Transform is the most effective of these methods for MCM. Thus, the figures presented herein will show the results from the S-Transform only. The S-Transforms of the vibrations from the healthy system are shown in Fig. 7. As can be seen, there is no particular pattern or evidence of any periodicity in the time–frequency domain in any of the spatial directions. The energy is confined to several bands but there seems to be no obvious structure to the distribution of the energy in those bands. The opposite is true for the spindle block vibrations when the positioning servo is at fault. This is illustrated in Fig. 8, which shows the S-Transform of the vibrations of a faulty system. It is immediately apparent that there is a periodic structure to the frequency content in the time–frequency representation. In each direction, there is a regular series of pulsations.

A major factor in the success of SRC is the choice of a suitable template. This, as explained in Section 2.2, is the feature against which all unknown signals will be compared. Clearly, the

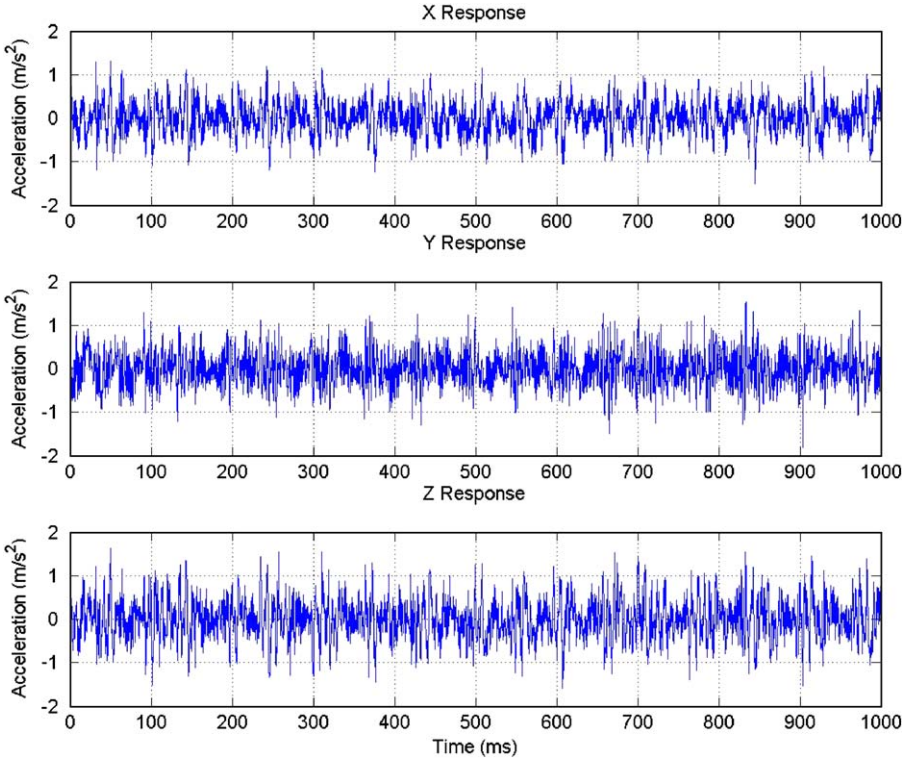

Fig. 5. Vibrations of the spindle block with a faulty positioning drive.

signature of the brush seizing fault is appropriate as a template signal because it has a definite, periodic structure, as seen in Fig. 8. The vibrations of a healthy system exhibit much less structured information, and are thus less effective as a template. Analysis has indicated that, if the vibrations of the healthy system are used as a template, it could lead to considerable numbers of false alarms. In such cases, the template and the measured signal can appear to be very different, even though they represent the same state. Furthermore, because the pattern generated by a brush seizing fault is the same irrespective of the feed rate used, and it is very distinctive from that of a healthy system, it makes an excellent template.

4. MCM using selective regional correlation

4.1. Performance measurement for SRC

As explained in Section 2.2, SRC works by comparing the windowed inverse time–frequency transform of unknown signal, $v_{U1}(t)$, to the template signals, $v_{Fi1}(t)$. Using Eq. (12), one can calculate ρ_i, the correlation coefficient between the unknown signal and the ith template. If $v_{U1}(t)$ matches with a specific $v_{Fi1}(t)$, the peak value of ρ_i will be high with respect to unity. The peak

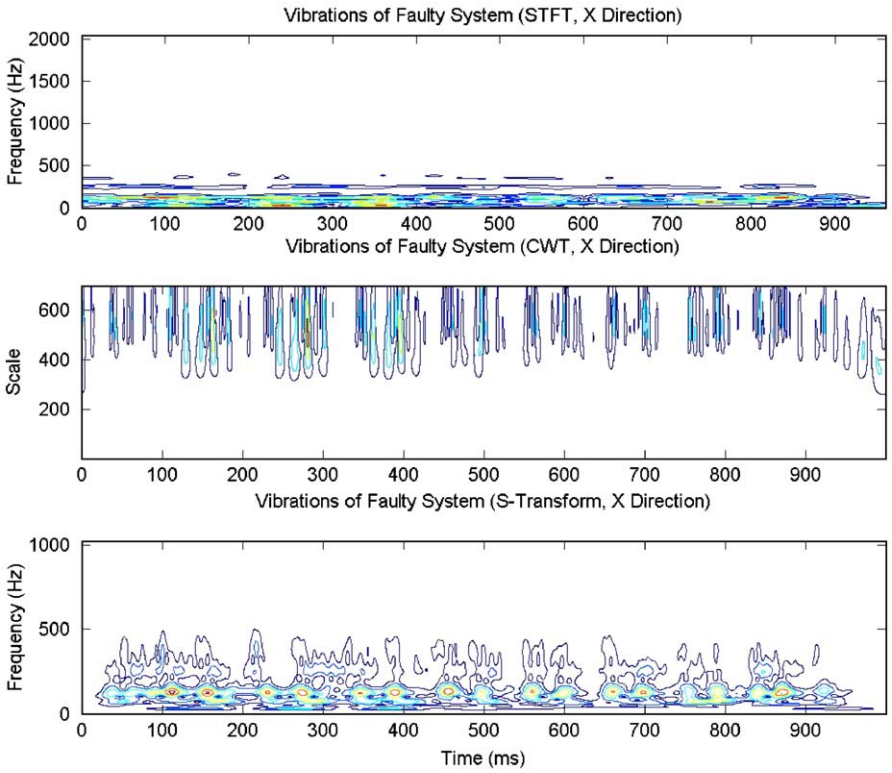

Fig. 6. Time–frequency representation of vibrations in the X direction using different transformations.

correlation coefficient generated in such cases, where the unknown and the template represent the same or similar phenomenon, is referred to as ρ_{similar}. On the other hand, if $v_{U1}(t)$ does not match a specific template, the value of ρ_i generated will be low. In this case, the correlation coefficient is known as $\rho_{\text{dissimilar}}$. Thus, it follows:

$$\rho_i = \rho_{\text{similar}} \quad \text{if } v_{U1(t)} \approx v_{Fi1(t)}, \tag{13}$$

$$\rho_i = \rho_{\text{dissimilar}} \quad \text{if } v_{U1(t)} \neq v_{Fi1(t)}. \tag{14}$$

Consequently, the correlation coefficients will have the following relationship:

$$\rho_{\text{similar}} > \rho_{\text{dissimilar}}. \tag{15}$$

This property can be used to determine the resolution of SRC-based pattern classification schemes. The resolution of the SRC scheme represents the difference between the correlation coefficients when the unknown signal represents a phenomenon similar to the template and when the unknown signal represents phenomenon dissimilar to the template. Thus, the resolution, φ, is defined as

$$\varphi = \rho_{\text{similar}} - \rho_{\text{dissimilar}}. \tag{16}$$

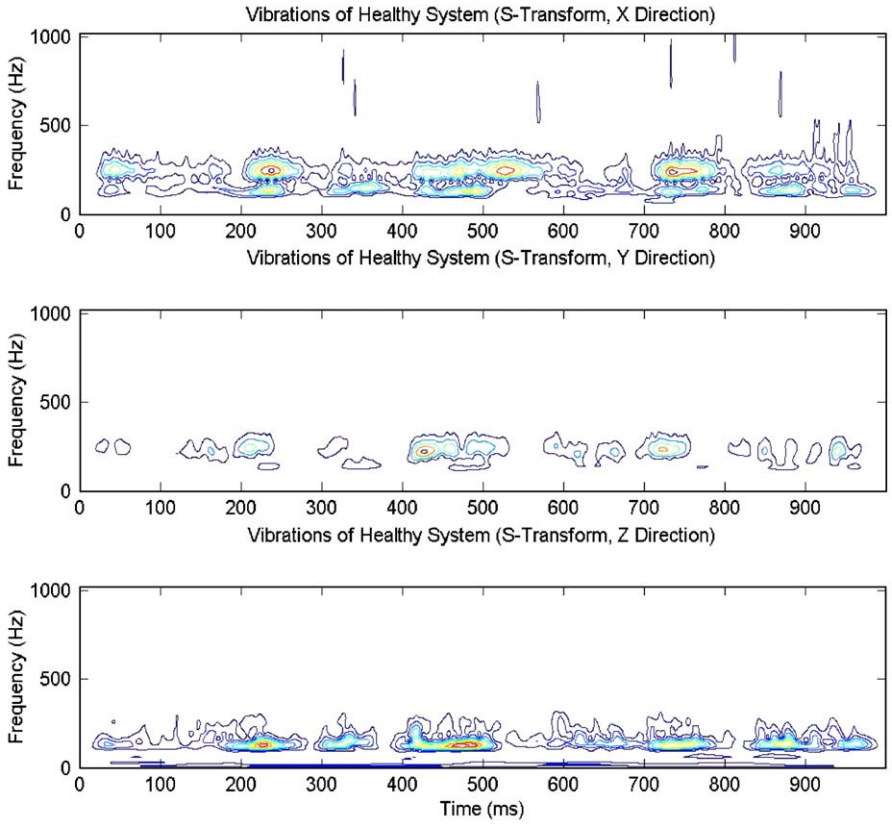

Fig. 7. S-Transform of healthy system in all spatial directions.

The values of ρ_{similar} and $\rho_{\text{dissimilar}}$ used to calculate the resolution may be from a single calculation or an average based on several measurements. In this paper, the resolution is based on averages of twelve tests performed under both healthy and faulty conditions.

In a functional MCM application, the unknown signal, $v_U(t)$, collected during machining, will be compared to the various templates, $v_{Fi}(t)$, using the method proposed herein. However, in this case, there will be no a priori knowledge about which state $v_U(t)$ represents. Thus, the magnitude of $\rho_i(\zeta)$ generated will be such that

$$\rho_i(\zeta) \in [\rho_{\text{dissimilar}}, \rho_{\text{similar}}]. \tag{17}$$

Consequently, it can be seen that if the peak value of $\rho_i(\zeta)$ is closer to the value of $\rho_{\text{dissimilar}}$, the unknown signal $v_U(t)$, will not be similar to the faulty signal $v_{Fi}(t)$, and then the system can be considered to be operating normally.

To correctly determine whether $v_U(t)$ corresponds to a particular $v_{Fi}(t)$, the distance, $\chi_i(\rho_i(\zeta), \rho_{\text{similar}})$, of $\rho_i(\zeta)$ from ρ_{similar} can be calculated:

$$\chi_i(\rho_i(\zeta), \rho_{\text{similar}}) = \|\rho_i(\zeta) - \rho_{\text{similar}}\|. \tag{18}$$

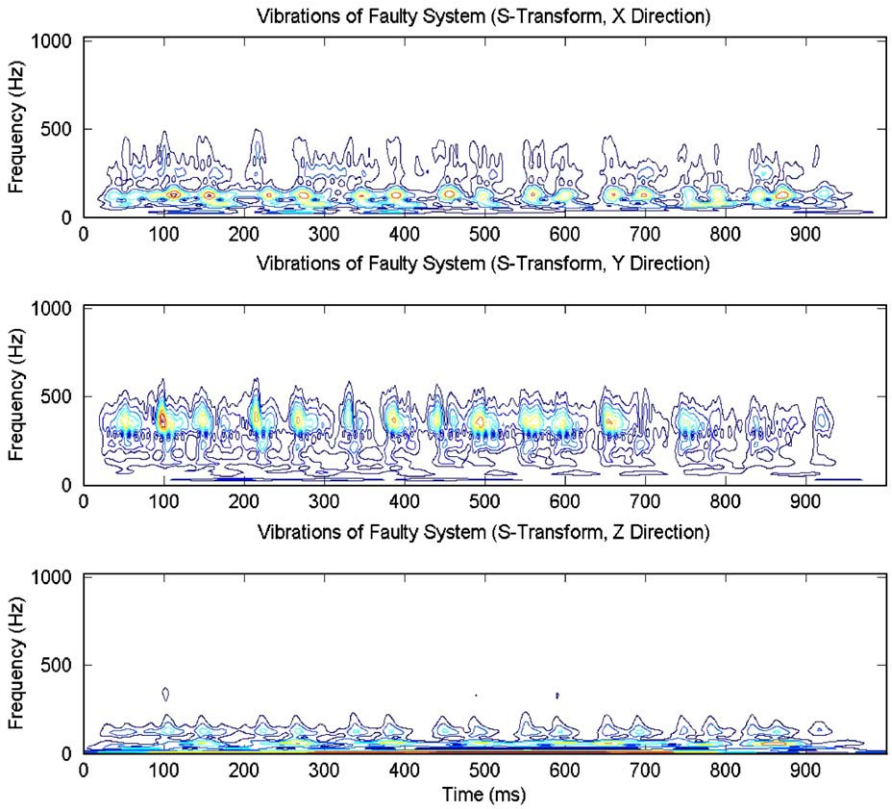

Fig. 8. S-Transform of faulty system in all spatial directions.

Using Eq. (18), the distance of $\rho_i(\zeta)$ from $\rho_{\text{dissimilar}}$, $\chi_i(\rho_i(\zeta), \rho_{\text{dissimilar}})$, can also be determined. The values of $\chi_i(\rho_i(\zeta), \rho_{\text{dissimilar}})$ and $\chi_i(\rho_i(\zeta),\rho_{\text{similar}})$ can then be compared, and a decision can be made as to whether or not the $v_U(t)$ being considered represents a specific fault. Obviously, if $\chi_i(\rho_i(\zeta)\rho_{\text{similar}}) > \chi_i(\rho_i(\zeta), \rho_{\text{dissimilar}})$, then $v_U(t)$ represents the specific fault condition represented by $v_{Fi}(t)$; otherwise, the system is assumed to be healthy. If the opposite is true, the conclusion can be made that $v_U(t)$ does not represent the specific fault under consideration.

4.2. Performance of fault detection using SRC

As stated earlier, time domain analysis may not offer conclusive results, but time–frequency domain analysis does. The STFT is performed using a Hamming window that is 60 ms in length, with an overlap of 50%. For the CWT, 70 voices are chosen, and the mother wavelet selected is a Gaussian wavelet. The S-Transform is performed according to the method described in [15].

Templates are selected using one of three 2D windows: a rectangular window, a Gaussian window or a Kaiser window. Each of the windows isolates a feature in the time–frequency domain which exists for a range $R = \{(\tau, \gamma) : \tau \in [540, 630\,\text{ms}], \gamma \in [20,\ 200\,\text{Hz}]\}$. For the Gaussian window, the best performance occurs when $\sigma_\tau = 31$ and $\sigma_\gamma = 50$. The Kasier window performs the best

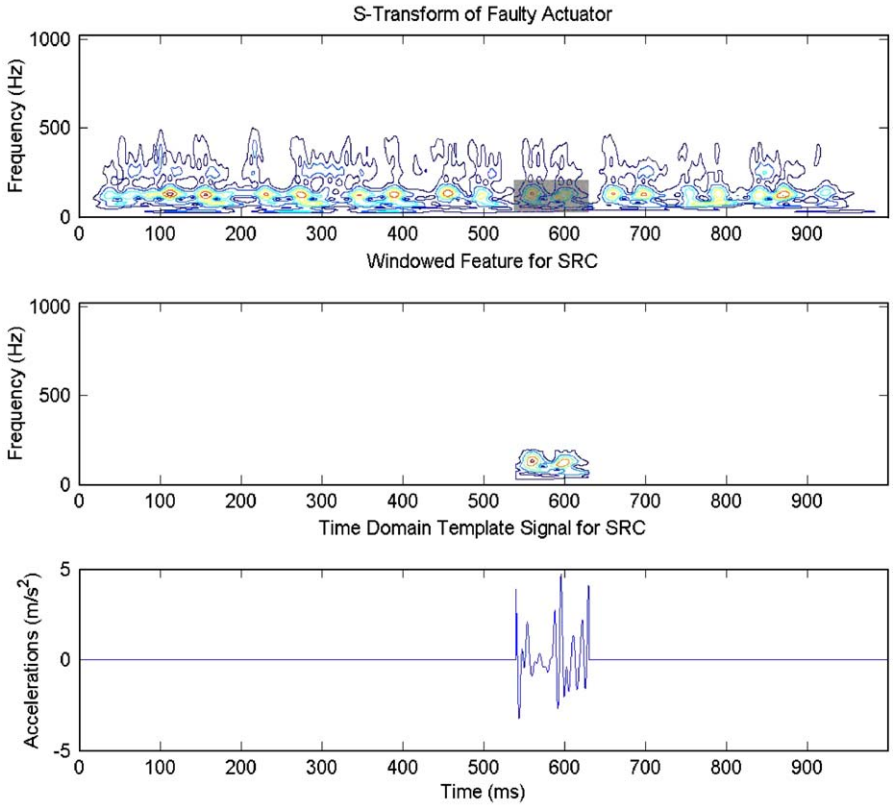

Fig. 9. Template signal selection from the S-Transform of a faulty drive.

when $\beta_\tau = 2.25$ and $\beta_\gamma = 2.25$. The selection of a specific template with the rectangular window in the X direction is shown in Fig. 9. The upper graph depicts the S-Transform of the entire vibration signal, $Tv_F(\tau, \gamma)$, and the shaded region on the graph represents the area covered by the 2D window. The middle graph displays the windowed and isolated feature of interest in the time–frequency domain, $Tv_{F1}(\tau, \gamma)$. The bottom graph shows the corresponding time domain signal, $v_{F1}(t)$, that is used in SRC. The three windows used are depicted in Fig. 10.

SRC improves the ability to distinguish between similar and dissimilar patterns beyond conventional correlation by improving the resolution for different states of the system. The results are presented in Tables 1–4. The values for ρ_{similar} and $\rho_{\text{dissimilar}}$ are average values over twelve tests. Tables 1–4 presents the performance of the considered time–frequency methods as well as the results obtained when conventional correlation is used.

The performance of SRC varies with the time–frequency method chosen, the 2D window used in feature isolation and the spatial direction considered. This can be seen by comparing the values of φ presented in Tables 1–3.

From these tables, several interesting observations can be made. The highest values of φ for a specified time–frequency method generally correspond to the Z direction, although this is not the case for the S-Transform. Also, changing the time–frequency method used has a more

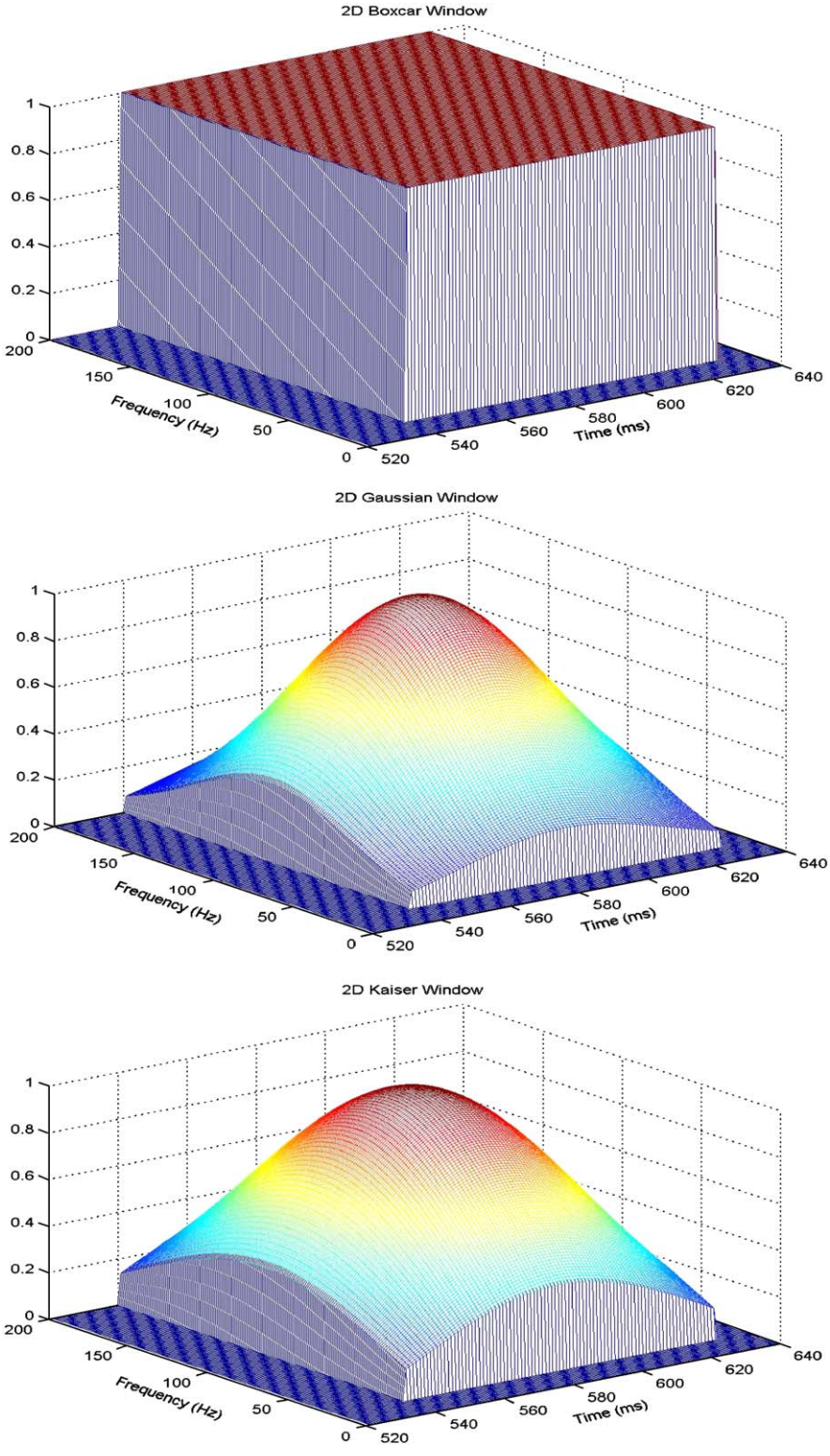

Fig. 10. The 2D windows used for numerical analysis.

Table 1
Performance of SRC using a 2D rectangular window

Direction	Selective regional correlation								
	STFT			CWT			S-Transform		
	X	Y	Z	X	Y	Z	X	Y	Z
ρ_{similar}	45.31	51.77	67.01	29.94	16.88	73.43	55.22	65.57	59.81
$\rho_{\text{dissimilar}}$	24.13	23.42	32.98	13.99	10.75	25.74	18.10	17.62	14.33
φ	21.18	28.35	34.03	15.95	6.13	47.69	37.12	47.95	45.48

Table 2
Performance of SRC using a 2D Gaussian window

Direction	Selective regional correlation								
	STFT			CWT			S-Transform		
	X	Y	Z	X	Y	Z	X	Y	Z
ρ_{similar}	48.36	55.21	69.18	34.67	19.78	79.60	58.47	69.51	62.30
$\rho_{\text{dissimilar}}$	31.41	30.64	38.49	22.06	14.89	39.65	27.68	25.24	28.51
φ	16.95	24.57	30.69	12.61	4.89	39.95	30.79	44.27	33.79

Table 3
Performance of SRC using a 2D Kaiser window

Direction	Selective regional correlation								
	STFT			CWT			S-Transform		
	X	Y	Z	X	Y	Z	X	Y	Z
ρ_{similar}	61.71	66.43	72.43	48.23	19.31	82.10	62.11	71.84	66.73
$\rho_{\text{dissimilar}}$	33.18	33.97	33.22	26.31	11.43	38.29	22.93	22.19	30.49
φ	28.53	32.46	39.12	21.92	7.88	43.81	39.18	49.65	36.24

pronounced effect on the resolution of the SRC result than does the shape and type of the window employed for feature extraction. It should also be noted that the S-Transform achieves the best resolution among all three time–frequency methods used, with the STFT coming second. The CWT has the poorest resolution of the three methods tested in X and Y directions, but its resolution is equal to, or even better than, the others in Z direction. Of the three windows considered, the Kaiser yields the highest resolution while the Gaussian window performs the worst.

It is very useful to compare the results obtained using SRC with those from conventional correlation. As can be seen, by comparing the values in Tables 1–3, with those in Table 4, the

Table 4
Performance of classifier using conventional correlation

Direction	Correlation		
	X	Y	Z
ρ_{similar}	6.52	5.60	10.02
$\rho_{\text{dissimilar}}$	5.81	2.85	5.36
φ	0.71	2.75	4.66

values generated by conventional correlation for similar events are much smaller than those calculated using time–frequency methods and SRC in a given direction. Conventional correlation sees similar events as having only 10% similarity at most, which is well below the value of $\rho_{\text{dissimilar}}$ seen by any of the time–frequency methods. This is mainly due to the non-stationary nature of the vibration signals under consideration. The resolution of conventional correlation is extremely poor also, and never exceeds 5%, while any combination of time–frequency method and 2D window with SRC results in very high resolution between the two states. Thus, an MCM system that relies on conventional correlation will not be able to perform as effectively as the one based on time–frequency methods and SRC.

5. Conclusion

In this paper, it has been established that SRC with time–frequency pre-processing can be an excellent way to perform MCM. The variable resolution and preservation of phase information associated with the S-Transform makes it the best method for highlighting and isolating features of interest in the time–frequency domain. The potential for SRC as an MCM method has been demonstrated by detecting a servo brush seizing fault in the Z-axis of a five-axis machining centre. In addition, the resolution of this method has been shown to be far superior to conventional correlation-based methods.

This work is significant because it shows that industrially viable sensors can be used to obtain sufficient information for MCM purposes. It also proves that SRC is superior to conventional correlation which implies that it has the potential to greatly improve fault diagnostic capability in MCM applications.

Acknowledgements

The authors express their gratitude to the following institutions and individuals for their support in this research: the Natural Sciences and Engineering Research Council of Canada (NSERC), AUTO 21, the Government of Ontario, the University of Western Ontario and the National Research Council of Canada's Integrated Manufacturing Technologies Institute (NRC-IMTI), with special thanks to Dr. Peter Orban.

References

[1] G. Byrne, D. Dornfeld, I. Inasaki, G. Ketteler, W. Konig, R. Teti, Tool condition monitoring (TCM)—the status of research and industrial applications, Annals of the CIRP 44 (2) (1995) 541–567.
[2] L. Rakowski, Monitoring improves machining up time and shop efficiency, [Online document], [accessed January 2004] Available HTTP: http://www.production-machining.com/articles/0903tb2.html.
[3] T. Fortin, F. Duffeau, Large generator vibration monitoring, Eighth International Conference on Electrical Machines and Drives, Robinson College, Cambridge, UK, 1997, pp. 155–160.
[4] W.Q. Wan, M.F. Golnaraghi, F. Ismail, Prognosis of machine health condition using neuro-fuzzy systems, Mechanical Systems and Signal Processing 18 (2004) 813–831.
[5] D. Kocur, R. Stanko, Order bispectrum: a new tool for reciprocated machine condition monitoring, Mechanical Systems and Signal Processing 14 (6) (2000) 871–890.
[6] W.J. Wang, P.D. McFadden, Application of the wavelet transform to early detection of gear failure by vibration analysis, Structural Dynamics and Vibration 52 (1993) 13–20.
[7] P.D. McFadden, J.G. Cook, L.M. Forster, Decomposition of gear vibration signals by the generalized S Transform, Mechanical Systems and Signal Processing 13 (5) (1999) 691–707.
[8] Z.K. Peng, F.L. Chu, Application of wavelet transform in machine condition monitoring and fault diagnostics: a review with bibliography, Mechanical Systems and Signal Processing 18 (2004) 199–221.
[9] P.J. McCully, C.F. Landy, Evaluation of current and vibration signals for squirrel cage induction motor condition monitoring, Eighth International Conference on Electrical Machines and Drives, 1–3 September, Cambridge, UK, 1997, pp. 331–336.
[10] E. Sejdić, J. Jiang, Selective regional correlation for pattern recognition, IEEE Transactions on Systems, Man and Cybernetics—Part A 2004, submitted and revised for publication.
[11] K. Grochenig, Foundations of Time–Frequency Analysis, Birkhauser, Boston, 2001.
[12] S. Mallat, A Wavelet Tour of Signal Processing, second ed., Academic Press, San Diego, 1999.
[13] I. Daubechies, Ten Lectures on Wavelets, Society for Industrial and Applied Mathematics, Philadelphia, PA, 1992.
[14] A.N. Akansu, R.A. Haddad, Multiresolution Signal Decomposition: Transforms, Subbands, and Wavelets, Academic Press, San Diego, London, 2001.
[15] R.G. Stockwell, L. Mansinha, R.P. Lowe, Localization of the complex spectrum: the S-Transform, IEEE Transactions on Signal Processing 44 (4) (1996) 998–1001.
[16] R. Pinnegar, The generalized S-Transform and TT-Transform, in one and two dimensions, Ph.D. Dissertation, The University of Western Ontario, London, Ont., September 2001.
[17] A.G. Rehorn, P.E. Orban, J. Jiang, Vibration-based machine condition monitoring with attention to the use of time–frequency methodologies, Intelligent Manufacturing, Proceedings of SPIE 5263 (2003) 10–21.
[18] L. Cohen, Time–Frequency Analysis, Prentice-Hall, PTR, Englewood Cliffs, NJ, 1995.
[19] A.G. Rehorn, J. Jiang, P. Orban, E.V. Bordatchev, Modelling and experimental investigation of spindle and cutter dynamics for a high-precision machining center, International Journal of Advanced Manufacturing Technology, doi: 10.1007/S00170-003-1794-8, 2003.